THE JOURNAL OF COMPARATIVE NEUROLOGY 489:11–22 (2005)

Expression of $GABA_B$ Receptor in the Avian Auditory Brainstem: Ontogeny, Afferent Deprivation, and Ultrastructure

R. MICHAEL BURGER,[1] JOSHUA D. PFEIFFER,[1] LESNICK E. WESTRUM,[2] AMY BERNARD,[1] AND EDWIN W RUBEL[1]*

[1]Virginia Merrill Bloedel Hearing Research Center and Department of Otolaryngology-Head and Neck Surgery, University of Washington, Seattle, Washington 98195

[2]Departments of Neurological Surgery and Biological Structure, University of Washington, Seattle, Washington 98195

ABSTRACT

Nucleus magnocellularis (NM), nucleus angularis (NA), and nucleus laminaris (NL), second- and third-order auditory neurons in the avian brainstem, receive GABAergic input primarily from the superior olivary nucleus (SON). Previous studies have demonstrated that both $GABA_A$ and $GABA_B$ receptors ($GABA_B$Rs) influence physiological properties of NM neurons. We characterized the distribution of $GABA_B$R expression in these nuclei during development and after deafferentation of the excitatory auditory nerve (nVIII) inputs. We used a polyclonal antibody raised against rat $GABA_B$Rs in the auditory brainstem during developmental periods that are thought to precede and include synaptogenesis of GABAergic inputs. As early as embryonic day (E)14, dense labeling is observed in NA, NM, NL, and SON. At earlier ages immunoreactivity is present in somas as diffuse staining with few puncta. By E21, when the structure and function of the auditory nuclei are known to be mature, $GABA_B$ immunoreactivity is characterized by dense punctate labeling in NM, NL, and a subset of NA neurons, but label is sparse in the SON. Removal of the cochlea and nVIII neurons in posthatch chicks resulted in only a small decrease in immunoreactivity after survival times of 14 or 28 days, suggesting that a major proportion of $GABA_B$Rs may be expressed postsynaptically or on GABAergic terminals. We confirmed this interpretation with immunogold TEM, where expression at postsynaptic membrane sites is clearly observed. The characterization of $GABA_B$R distribution enriches our understanding of the full complement of inhibitory influences on central auditory processing in this well-studied neuronal circuit. J. Comp. Neurol. 489:11–22, 2005.

Indexing terms: inhibition; deafferentation; chicken; auditory system; development; immunohistochemistry

Sensory processing involves computations among parallel and serial networks of neurons. These networks utilize the convergence of excitatory and inhibitory inputs to extract relevant features of the external environment. The avian brainstem auditory system is a well-characterized sensory network composed of four pairs of nuclei, where ascending excitatory afferents interact with descending GABAergic efferents (Rubel et al., 2004). The predominant source of GABAergic input in the avian auditory brainstem is the superior olivary nucleus (SON) (Carr et al., 1989; Lachica et al., 1994; Yang et al., 1999), but a small population of neurons residing in the neuropil of nucleus magnocellularis (NM) and nucleus laminaris (NL) also provide GABAergic input (von Bartheld et al., 1989). The SON projects ipsilaterally to both nucleus angularis (NA) and NM, divisions of the avian cochlear nuclei, as well as to NL, a binaural nucleus, where interaural time disparities are computed (Parks and Rubel, 1975; Conlee

Grant sponsor: National Institutes of Health/National Institute on Deafness and Other Communication Disorders; Grant number: DC00395; Grant number: DC04661; Grant number: DC00466

*Correspondence to: Edwin W Rubel, Box 357923, University of Washington, Seattle WA, 98195-7923. E-mail: rubel@u.washington.edu

Received 29 September 2004; Revised 8 February 2005; Accepted 7 March 2005

DOI 10.1002/cne.20607

Published online in Wiley InterScience (www.interscience.wiley.com).

and Parks, 1986; Lachica et al., 1994; Westerberg and Schwarz, 1995; Yang et al., 1999; Burger et al., 2005). A separate SON projection innervates the contralateral SON (Burger et al., 2005).

The GABAergic input to neurons of both NM and NL via ionotropic $GABA_A$ receptors generates a potent inhibition through a depolarizing Cl^- conductance that has been suggested to influence action potential timing and coincidence detection (Hyson et al., 1995; Funabiki et al., 1998; Yang et al., 1999; Lu and Trussell, 2000, 2001; Monsivais et al., 2000; Monsivais and Rubel, 2001). $GABA_B$ receptors ($GABA_BRs$) are known to mediate a broad range of metabotropic effects, but typically modulate G-protein–coupled K^+ channels postsynaptically and voltage-gated Ca^{++} conductances presynaptically (for review, see Kerr and Ong, 1995; Calver et al., 2002). Recent studies have established that GABAergic influences in NM are also mediated by $GABA_BRs$ (Brenowitz et al., 1998; Brenowitz and Trussell, 2001; Lu et al., 2004). These studies demonstrate that activation of $GABA_BRs$ can modulate release of transmitter presynaptically from both excitatory and inhibitory terminals.

In the chicken auditory system the developmental time course of GABAergic innervation has been well characterized (Code et al., 1989). On the basis of immunohistochemistry, Code et al. (1989) observed innervation and synaptogenesis of GABAergic inputs to NM taking place between embryonic day (E)12 and E17. Synaptic physiological studies in our laboratory confirm this basic timeline (unpubl. obs.).

This report represents one component of a broader effort to understand the roles of inhibitory input in information processing and development of the avian brainstem auditory system. We utilized an antibody raised against a peptide sequence common to two of the known isoforms of the rat $GABA_BR1$ subunit, $GABA_BR1a$ and $GABA_BR1b$ (see Materials and Methods), to characterize expression in the chick auditory brainstem during development, following afferent deprivation, as well as in the normal mature system. Additionally, we analyzed $GABA_BR$ expression at the ultrastructural level in NM to determine its specific subcellular and synaptic membrane localization in NM.

MATERIALS AND METHODS

Tissue preparation

This report is based on tissue from 24 embryonic and 20 posthatch inbred White Leghorn chickens. All animal care and euthanasia procedures conformed to protocols approved by the University of Washington Institutional Animal Care and Use Committee and to NIH guidelines. Embryonic tissue was harvested by partial extraction of embryos from the egg followed by rapid decapitation. The skull was opened and heads were then submerged for 24 hours in 4% paraformaldehyde in 0.1 M phosphate-buffered saline (PBS), pH 7.4, at 4°C. Posthatch animals were administered a lethal dose by intramuscular injection of sodium pentobarbital prior to transcardial perfusion with PBS containing heparin (1,000 units/L) for 2–5 minutes. Washout was followed by 4% paraformaldehyde in PBS for 5–10 minutes. After craniotomy, tissue was then postfixed for 4–24 hours at 4°C. Coronal sections were made at 12 μm on a cryostat or at 50 μm on a vibratome through the rostrocaudal extent of the auditory brainstem. For cryostat sections, brains were first cryoprotected in 30% sucrose in PBS overnight, then blocked and embedded in Tissue Tek OCT (Sakura Finetek, Albertville, MN). Cryostat sections were mounted on gelatin-coated slides for immunohistochemistry (IHC). Vibratome sections were collected into vials containing PBS for IHC and then mounted. All chemicals were purchased from Sigma Chemical (St. Louis, MO) unless otherwise stated.

Immunohistochemistry

We used a polyclonal antibody against the peptide sequence PSEPPDRLSCDGSRVHLLYK common to both rat $GABA_BR1a$ and $GABA_BR1b$ subunits (AB1531, Chemicon, Temecula, CA) diluted to 1:500 or 1:1,000 in a blocking solution of 4% normal goat serum 0.1% Triton-X in PBS. First, endogenous peroxidases were quenched by immersion of sections in a solution of 0.6% H_20_2 in methanol for 5 minutes followed by a rinse in PBS. Tissue was then blocked for 1 hour. After blocking, sections were incubated with primary antisera for 24 hour at 4°C. The tissue was thoroughly rinsed, then incubated with secondary antibody solution of biotinylated goat anti-guinea pig IgGStrong (Vector Laboratories, Burlingame, CA) at 1:200 in block. After rinsing, the tissue was incubated in avidin-biotin peroxidase complex for 1 hour. Tissue was reacted for 1–2 minutes with diaminobenzidine solution (DAB) (0.357 mg/ml DAB in 0.03% H_2O_2 in PBS). Tissue was then dehydrated in ethanol, cleared in xylenes, and coverslipped in DPX (Electron Microscopy Sciences, Fort Washington, PA).

Antibody validation and Western blotting

Since this is the first study we are aware of using this antibody in avian tissue, we conducted several controls to test antibody specificity in this species. First, Figure 1A illustrates the strong specific immunoreactivity in Purkinje cells of the chicken cerebellum consistent with staining in mammalian preparations (Fritschy et al., 1999). Figure 1B shows low background staining in an alternate section that was not exposed to primary antibody. We conducted a Western blot immunoassay to confirm that this antibody probed similar proteins in chicken compared to mammals. Western blotting was repeated three times on two separate sets of tissue and was conducted using the method adapted from Benke et al. (1996). P4 chicken ($n = 4$) and P42 ($n = 5$) mouse brains were dissected and immediately frozen to −80°C. In chickens, tissue was derived from dissection of the region of NM and NL or from the cerebellum. A membrane preparation was prepared as follows: Tissue was homogenized (Polytron PT1200, Kinematica, Switzerland) for 3×5 minutes on ice in Extraction Buffer (10 mM Tris-HCl pH 7.4, 320 mM sucrose, 5 mM EDTA pH 8.0, 100 μM PMSF, and Complete Protease Inhibitor [Roche, Basel Switzerland]). Solubilized tissue was then centrifuged for 20 minutes at 4°C, 16,000*g*, and the resulting pellet was resuspended in an equal volume of extraction buffer and spun as before (3×). The pellet was resuspended in extraction buffer and protein content of the crude membrane suspension was quantified (BCA kit, Pierce, Rockford, IL). An equal volume of Sample Buffer (125 mM Tris-HCl, pH 8.0, 20% glycerol, 0.0002% bromophenol blue, 10% 2-β-mercaptoethanol, 4% SDS) was added to each sample and samples were heated to 95°C for 5 minutes. Comparable amounts of protein (~60

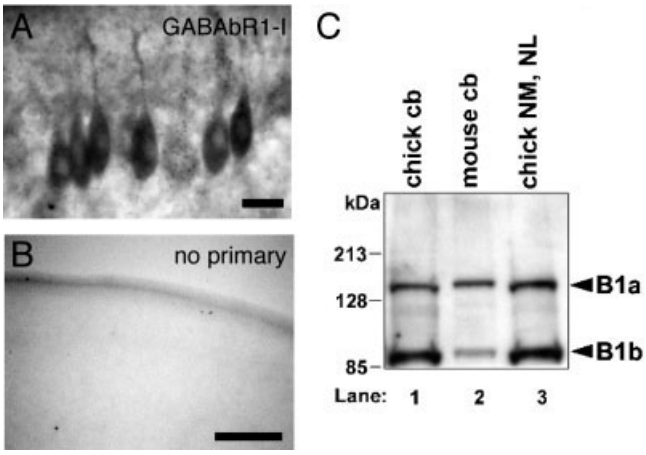

Fig. 1. Antisera raised against rat GABA$_B$R-1 recognizes chicken GABA$_B$R-1. **A:** High-magnification photomicrograph of a 50 μm section through the cerebellum where strong labeling of Purkinje cells is clearly visible. **B:** Very little nonspecific background staining in an alternate section at lower magnification prepared with no primary antibody. **C:** The results of a Western blot assay that included tissue from chicken cerebellum (Lane 1), mouse cerebellum (Lane 2), and chicken NM/NL (Lane 3). Molecular weight standards (left) were used to determine relative sizes of labeled protein. Chicken reactivity is nearly identical to that in the mouse with respect to the molecular weights of the two visible bands corresponding to GABA$_B$R1a and GABA$_B$R1b splice variants. Scale bar = 20 μm in A; 100 μm in B.

μg per lane) were then separated by PAGE on a 12% Tris-HCl acrylamide gel (BioRad, Hercules, CA). Proteins were transferred by electrophoresis to PVDF membrane (BioRad). Subsequent immunodetection was performed according to the manufacturer's instructions, using anti-GABA$_B$R1, at a concentration of 1:500. A secondary HRP-conjugated rabbit anti-guinea pig antibody (Zymed, San Francisco, CA) was used at a concentration of 1:3,000. Proteins were visualized by ECL (Amersham, Buckinghamshire, UK). The results shown in Figure 1C illustrate nearly identical band recognition between chicken and mouse. The two bands in each lane correspond to the two GABA$_B$R1 subtypes previously identified with this antibody (Fritschy et al., 1999).

Electron microscopic immunocytochemistry

Two P3 chickens were perfused and postfixed with cold 4% paraformaldehyde and 0.1% glutaraldehyde in PBS. Coronal sections were cut at 100 μm on a vibratome. All incubations were at 4°C and for 48 hours. The secondary antibody was conjugated to 1 nm colloidal gold (Nanoprobes, Yaphank, NY) and diluted to 1:50. Following incubation with secondary and rinse, tissue was again fixed in 2% glutaraldehyde for 10 minutes. Tissue was rinsed in PBS then in ddH_2O for 5 × 10 minutes. Silver enhancement solution (R-Gent SE-EM Enhancement, Aurion, The Netherlands) was prepared according to the company's specifications and tissue was incubated for 30 minutes. The tissue was again rinsed in ddH_2O, then in 0.1 M PB. The 2% glutaraldehyde followed by ddH_2O rinse step was repeated. The sections were then osmicated in 1% osmium tetroxide for 15 minutes and rinsed in PB. Sections were dehydrated and embedded in Spurr's resin. Ultrathin sections of 90 nm were cut, collected on copper grids, and stained with uranyl acetate and lead citrate. Pioliform (Ted Pella, Redding, CA) coated slot grids and 200-mesh uncoated grids were used. A Philips CM 10 electron microscope was used to view the sections and for electron photomicroscopy.

Deafferentation

Unilateral basilar papilla removal was performed on nine P5 chickens as previously described (Born and Rubel, 1985). The cochlear ganglion was also removed by aspiration through the oval window. Following surgery, normal saline-treated gel foam was inserted into the cochlear duct and middle ear while the outer ear was closed with cyanoacrylate. The animals survived for 2 (n = 6) or 4 (n = 3) weeks before perfusion and immunohistochemistry. The 4-week survival animals were also used for quantitative analysis of GABA$_B$R expression between the deafferented and contralateral side of the brainstem. For this analysis, NM neurons were randomly selected by the following criteria: 1) they were completely contained within the section; 2) not adjacent to the border of NM; and 3) the whole cell and nucleus could be observed using Nomarski optics. High-power images of selected neurons were acquired in the plane of focus where the nucleus appeared widest. Using Object Image 2.11 (NIH) software, the plasma membrane and nuclear borders of individual cells were circumscribed and the nuclear area was excluded from analysis. Average pixel intensity was measured for the remaining cytosolic region. Images from all NM neurons meeting the above criteria in a given section were acquired with identical optical settings. Average pixel intensity scores for a sample of cells (range = 14–23) from control and deafferented sides of single sections from each animal (n = 3) were then compared. Mean control and deafferented scores for each animal were compared using unpaired *t*-tests.

Imaging

Photomicrographs were acquired using brightfield on a Zeiss Axioplan microscope using a Photometrics CoolSnap camera (Roper Scientific, Tucson, AZ) with Slidebook acquisition software (Intelligent Imaging Innovations, Denver, CO). Occasionally, blue filters were used to enhance contrast. For some images, pixel value histograms were stretched to maximize dynamic range for ease of comparison and quality of appearance.

RESULTS

In order to thoroughly characterize the localization and expression of GABA$_B$Rs, we analyzed chicken brainstem nuclei under several conditions. We first illustrate the mature expression pattern and then compare the mature pattern to that observed during development. In order to assess the presence of GABA$_B$Rs on postsynaptic or inhibitory elements, we then describe expression in NM following nVIII deafferentation and degeneration. Finally, we confirm postsynaptic expression at the ultrastructural level, where expression was observed on several synaptic elements in NM and NL.

Expression in the mature system

GABA$_B$R immunoreactivity (GABA$_B$R-I) was observed in all four brainstem auditory nuclei in 11 animals between ages E21–P4 (E21, n = 4; P1, n = 3; P4, n = 4), an

age range where the auditory system is considered to be mature (Rubel, 1978). Figure 2A,B shows low-power images of adjacent 50-μm vibratome Nissl-stained (2A) and $GABA_BR$-I reacted (2B) sections through P4 auditory brainstem. Figure 2B shows the strong and specific labeling of neurons in NM and NL nuclei. At high power, granular, punctate labeling is prominent in NM, NL, and NA neurons (Fig. 2C–E, respectively). $GABA_BR$-I can be observed extending away from NL somas into the NL's dendritic fields (arrow in 2D). Although recent studies have identified a diversity of cell types in NA (Hausler et al., 1999; Soares and Carr, 2001; Soares et al., 2002), due to the punctate nature of the label it is difficult to determine whether a subset or all of the identified neuron types in NA express $GABA_BRs$. In all three nuclei $GABA_BR$-I appears limited to neurons; in no case did we observe convincing labeling of glial cell bodies or processes. In contrast to NM, NA, and NL, $GABA_BR$-I labeling in the predominantly GABAergic SON is sparse. Immunoreactivity is lighter within SON than in the neurons surrounding this nucleus and the density of puncta is very low in high-power images (Fig. 2F).

Expression in the developing system

Metabotropic $GABA_BRs$ are known to influence development and maintenance of central synapses (Owens and Kriegstein, 2002). Here we characterized the expression pattern of $GABA_BRs$ through the developmental ages associated with synaptogenesis of both glutamatergic and GABAergic inputs to the brainstem auditory nuclei. The early developmental expression pattern was similar for all four nuclei (NM, NL, NA, and SON), with the notable exception of a decrease in $GABA_BR$-I in the SON at late stages. We processed tissue at the following ages: E8–9 (n = 2); E10 (n = 9); E11 (n = 3); E12 (n = 3); E14, (n = 5); E18 (n = 2); E21 (n = 4); P1 (n = 3); and P4 (n = 4). We present data in Figures 3–7 for NM, NL, NA, and SON, respectively, at E10, E14, and E21, ages that illustrate the major developmental changes we observed.

E8–11. At this early developmental phase the best evidence available suggests innervation and synaptogenesis of inhibitory terminals in NA, NM, and NL has not occurred (Code et al., 1989; and unpubl. obs.). Synaptogenesis of excitatory nVIII input to NM and of NM input to NL appears to occur during this period (Jhaveri and Morest, 1982; Rubel and Parks, 1988). $GABA_BR$-I is present mainly as diffuse dark staining throughout the immature somas of neurons in all four nuclei as early as E8. By E10, a few puncta can be observed on membrane surfaces. This pattern is observable in Panel A of Figures 3–6 and is consistent among all four nuclei. The staining is specific, as control sections processed without primary antibody is free of staining.

E12–14. Over the course of these 3 days invading inhibitory projections begin to develop varicosities that resemble preterminal axonal swellings, but identifiable GABAergic terminals on their targets in NM and NL are rare (Code et al., 1989). GABAergic synaptic events can be first detected reliably on E14 (unpubl. obs.). Coincident with these events, the number of immunoreactive puncta in all four nuclei increased dramatically, as shown in Figures 3–6, Panel B. At this age the diffuse somatic labeling remains, and is particularly well exemplified by Figure 4B.

E18–21. By E18 the anti-GABA immunoreactivity in NM and NL has acquired a mature pattern, with fewer GABAergic fibers but many GABA immunoreactive terminals surrounding neurons in NM and NL (Code et al., 1989). In NM, NA, and NL, $GABA_BR$-I is expressed as dense punctate labeling that appears to be both on the plasma membrane and throughout the cytoplasm. In contrast, label in SON neurons appears markedly reduced relative to levels observed at E14. In addition, the diffuse somatic staining that prevailed during earlier developmental stages is virtually absent in all four nuclei by E18 and thereafter.

Expression along the tonotopic axis

The frequency range of the auditory system of chickens spans about 10–5,000 Hz (Rubel and Parks, 1975; Warchol and Dallos, 1990). Neurons in NM and NL express several features that vary systematically along the tonotopic axis (Rubel and Parks, 1988; Fukui and Ohmori, 2004) across the roughly caudal to rostral tonotopic gradient, including density of inhibitory terminals (Code et al., 1989). From observations of coronal serial sections, we did not detect any gradient of immunoreactivity for $GABA_BRs$ along the main (caudolateral to rostromedial; Rubel and Parks, 1975) tonotopic axis of NM and NL. To verify this finding we sectioned two P1 brains parallel to the tonotopic axis through NM and NL. In all sections, high and low best frequency neurons were similar in terms of $GABA_BR1$ expression. Figure 7 shows a low-magnification para-tonotopic section through NL in 7A, along with corresponding high-power photomicrographs of high, middle, and low-frequency NL neurons in Figure 7B–D, respectively. Dense punctate label is observed uniformly across the tonotopic axis in both NM and NL.

Influence of afferent deprivation

It is known that $GABA_BR$ expression in NM is located on both the terminals of nVIII and GABAergic fibers (Otis and Trussell, 1996; Brenowitz et al., 1998; Brenowitz and Trussell, 2001; Lu et al., 2004). Since nVIII fibers are likely be a major source of $GABA_BR$-I, we investigated whether $GABA_BR$ expression changes following removal of the excitatory input to NM. We unilaterally removed the basilar papilla and cochlear ganglion in nine animals at P5. After survival times of 14 (n = 6) or 28 (n = 3) days, in Nissl-stained sections, we observed features typical of deafferented NM including eccentric nuclei, reduced neuron size, and an apparent reduction in neuron number (Born and Rubel, 1985).

Surprisingly, loss of nVIII fibers resulted in only a small difference in the density of $GABA_BR1$-I puncta in NM between control and deafferented sides of the brain; one representative case is shown in Figure 8. Panel A shows $GABA_BR$-I on the control side, while Panel B shows the contralateral deafferented NM. Measurements of average pixel intensity from random samples of NM somas from three brains revealed that while NM soma area was reduced on average by 27.7%, as expected (Fig. 8D), the average pixel intensity was only slightly reduced (Fig. 8C). In each of the three brains analyzed, average pixel intensity was consistently but only slightly reduced on the deafferented side compared to that on the control side. Unpaired *t*-tests from each brain confirmed the small changes were statistically significant in two of the three cases ($P = 0.01, 0.04$) and

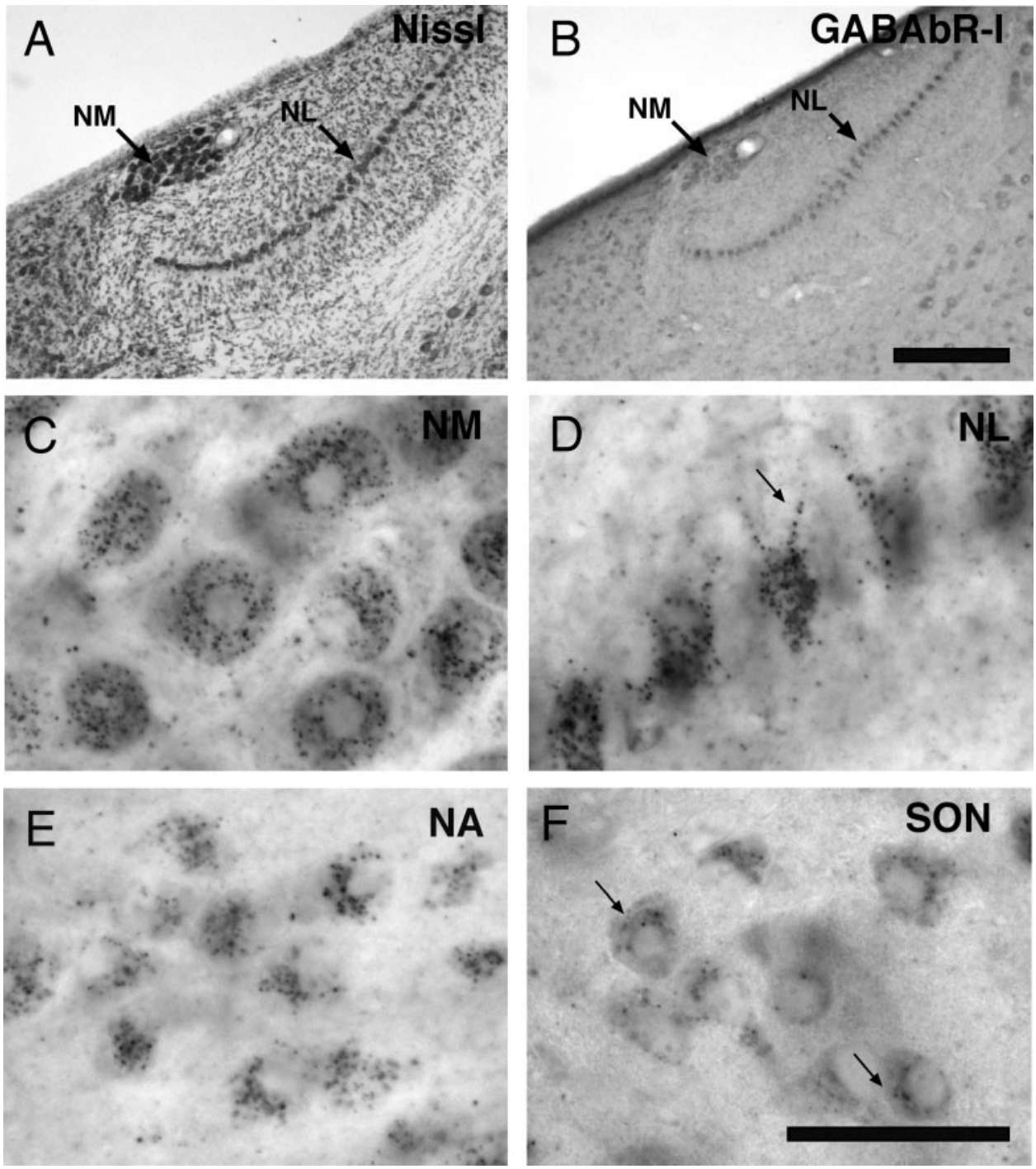

Fig. 2. GABA$_B$R-I in the mature chick auditory brainstem. **A,B:** Low-power photomicrographs of Nissl (A) and GABA$_B$R-I (B) stained adjacent vibratome sections through NM and NL of a P4 chicken. GABA$_B$R-I is abundant in both nuclei but staining is relatively absent in the glia enriched neuropil zones surrounding each nucleus. **C–E:** High-power images of NM (C), NL (D), and NA (E) neurons. GABA$_B$R-I has a dense granular appearance that appears largely restricted to the plasma membrane over the somatic area of the neurons. On NL neurons staining often appears to extend onto the dendrites (arrow in D). **F:** High-power image of staining in SON. In contrast to the other brainstem auditory nuclei, the staining in SON is markedly sparse. A few granules of immunoreactivity are present on most neurons (arrows). Scale bars = 100 μm in A (applies to A,B); 20 μm in F (applies to C–F).

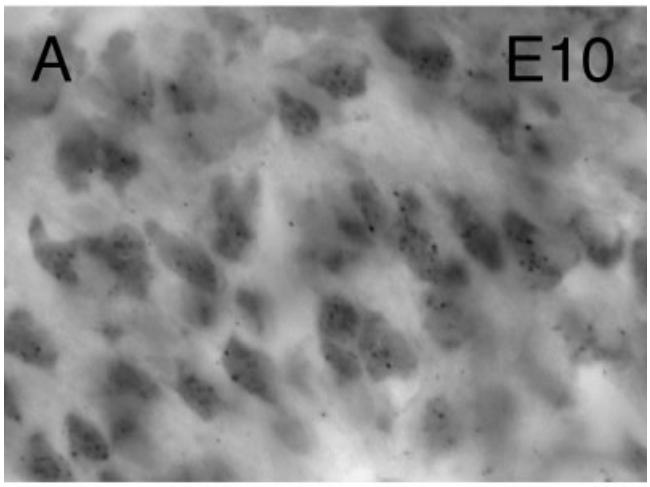

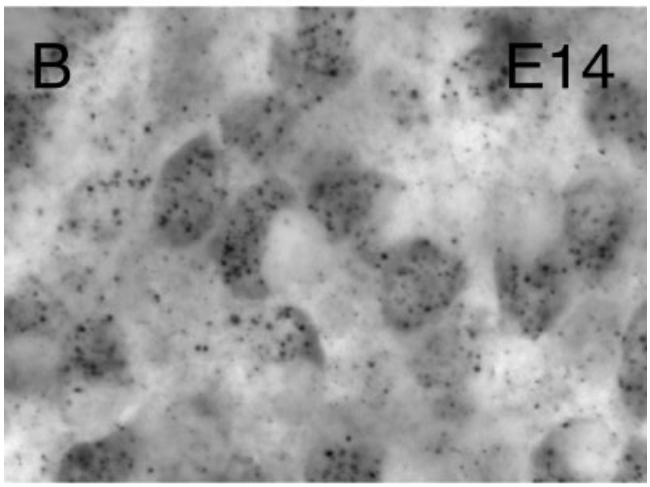

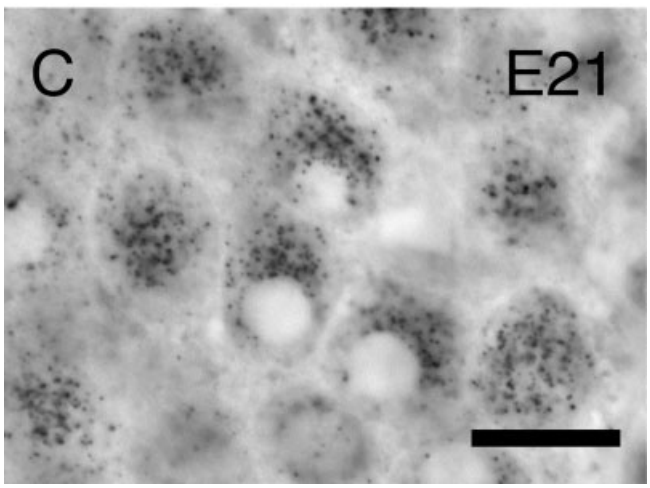

Fig. 3. Developmental pattern of $GABA_BR$-I expression in NM. **A:** At early ages $GABA_BR$-I staining is dominated by diffuse labeling in NM somas and few puncta are observable. **B:** By E14 punctate staining is dense, but diffuse cytosolic staining remains high. **C:** By E18, when most features of NM are mature, $GABA_BR$-I staining has a predominantly strong punctate granular appearance. The diffuse cytosolic staining that was observed at earlier ages is largely absent. Scale bar = 10 μm in C (applies to A–C).

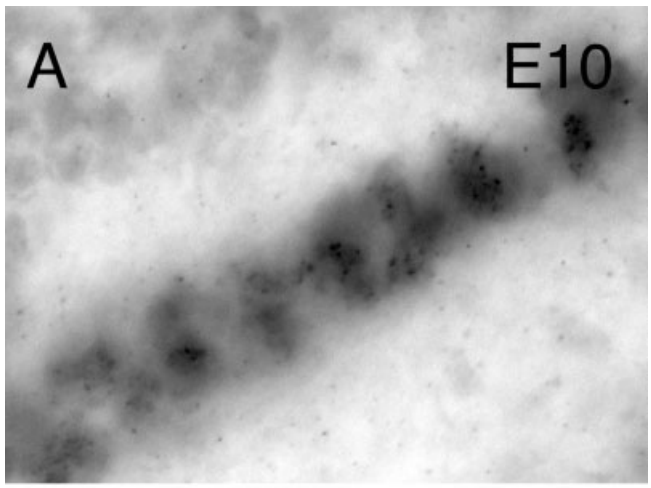

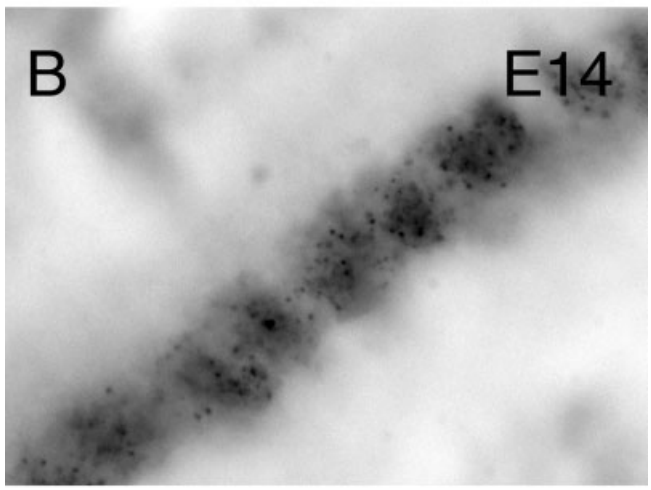

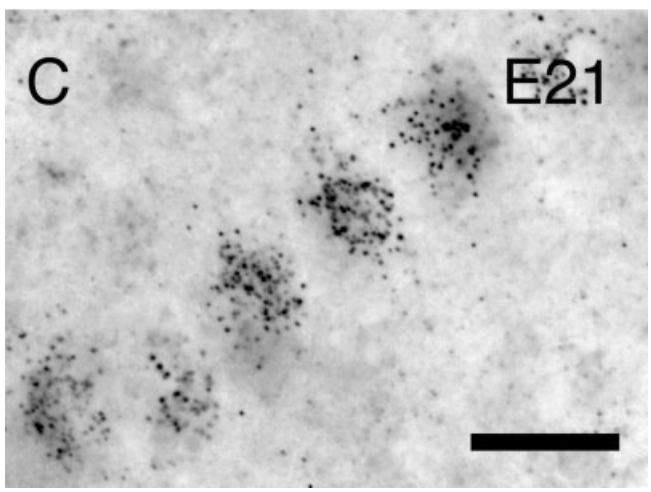

Fig. 4. Development of $GABA_BR$-I in NL. Details are the same as those for NM in Figure 3. Scale bar = 10 μm in C (applies to A–C).

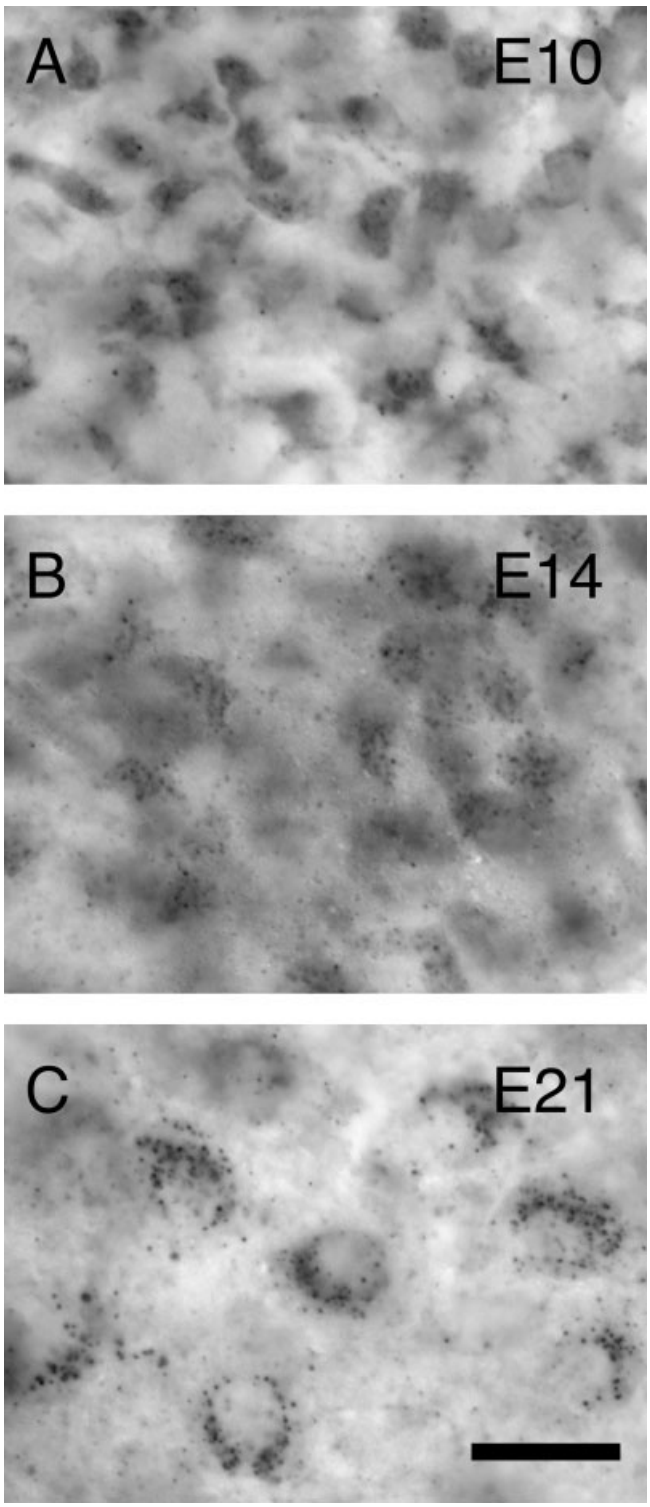

Fig. 5. Development of GABA$_B$R-I in NA. Details are the same as those for NM in Figure 3. Scale bar = 10 μm in C (applies to A–C).

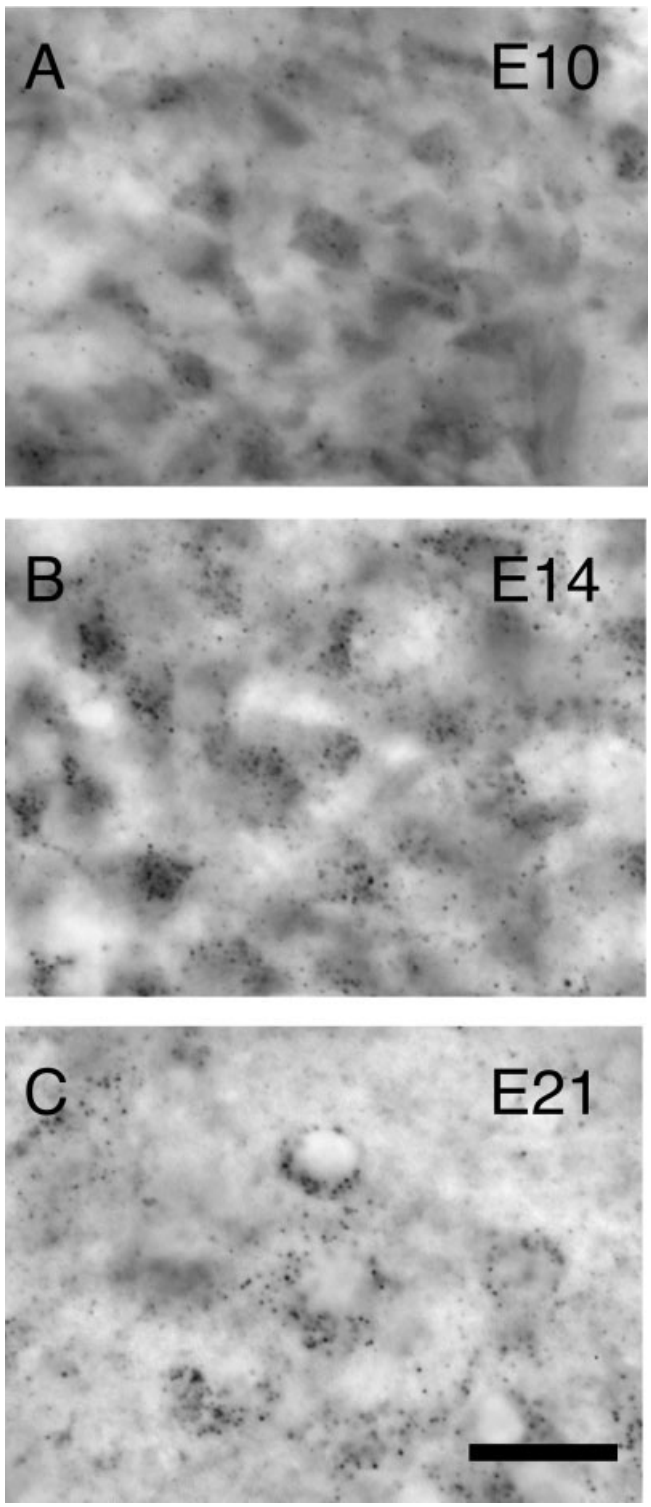

Fig. 6. GABA$_B$R expression peaks around E14 in the SON. Development of GABA$_B$R-I staining proceeds similarly to that observed in other brainstem nuclei at E10 (**A**) and E14 (**B**). However, by E18 (**C**) the staining is markedly reduced and remains so into maturity. Scale bar = 10 μm in C (applies to A–C).

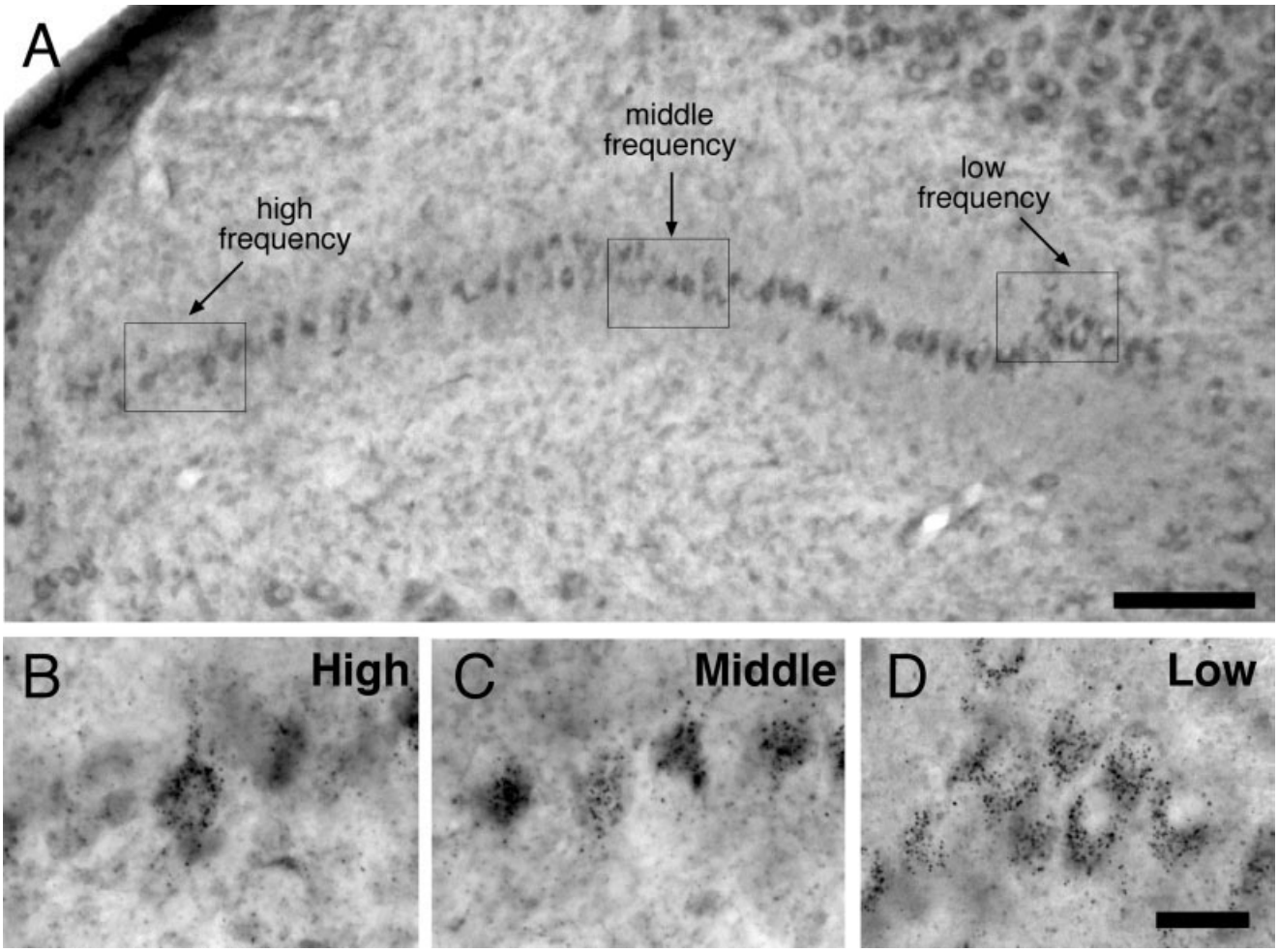

Fig. 7. $GABA_BR$-I does not vary with tonotopic position. **A:** A para-tonotopic section through NL and three highlighted frequency zones boxes. **B–D:** At high magnification the strong labeling apparent on NL cells regardless of position. Titles indicate relative tonotopic position. Scale bars = 100 μm in A; 20 μm in D (applies to B–D).

not significant in the other ($P = 0.54$). These data suggest that the that $GABA_BR$ expression in NM is independent of excitatory input and that the majority of $GABA_BRs$ expressed in NM reside on either GABAergic terminals or on NM cell membranes.

Preembedding immunocytochemical electron microscopy

The high expression of $GABA_BR$-I remaining 4 weeks after deafferentation suggested that postsynaptic expression in NM was a likely source of immunoreactivity. We sought to confirm this possible expression in NM using preembedded immunogold transmission electron microscopy preparations from two animals. We observed postsynaptic labeling that was clearly associated with NM membranes in the vicinity of Type II synaptic contacts with presynaptic pleomorphic vesicles (Fig. 9A). Figure 9B,C shows gold particle labeling was also observed proximal to apparent postsynaptic specializations of increased density and cleft space at putative excitatory terminals. Although these are preliminary electron microscopic observations, they confirm the presence of $GABA_BRs$ on NM neurons at both putative excitatory and inhibitory loci.

DISCUSSION

The data reported here support three main conclusions regarding the expression of $GABA_BRs$ in the avian auditory system. First, $GABA_BR1$ subunits are highly expressed in the mature NM, NA, and NL, and only weakly in the SON. This expression appears uniform along the tonotopic axes in NM and NL. Second, expression of $GABA_BR1$ is detectable at developmental stages that precede functional innervation by GABAergic inputs. Third, a high level of expression following deafferentation as well as our ultrastructural observations strongly suggest that $GABA_BR1$ receptor expression is present on postsynaptic NM neurons, in addition to the known $GABA_BR$ expression on nVIII terminals and GABAergic fibers that have been previously identified in physiological studies. In the following sections

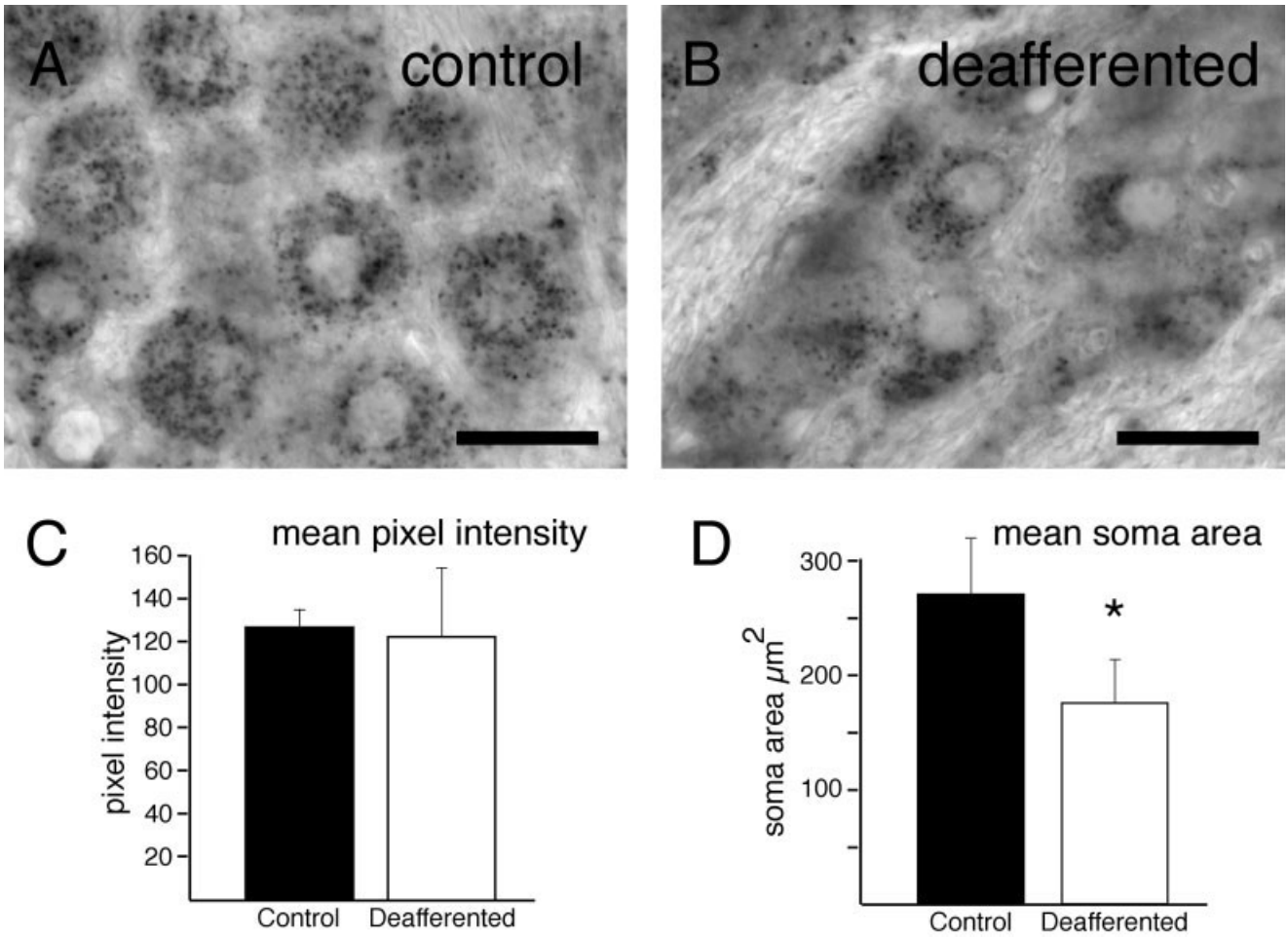

Fig. 8. GABA$_B$R-I decreases slightly following deafferentation. **A,B:** High-power images of NM in an animal that survived 4 weeks following basilar papilla and ganglion cell removal. NM cells exhibit several hallmarks of deafferentation, including reduced soma size and eccentrically positioned nuclei. **C:** The mean ± SD pixel intensity from neurons on the control (black bar) and deafferented (white bar) sides. The small difference in pixel intensity between the control and deafferented sides was not significant in this case ($P = 0.05$). **D:** The reduction in cell area is observed on the deafferented side (white bar), compared to control (black bars), the difference is highly significant ($P = 0.01$). Scale bars = 10 μm in A,B.

we expand on each of these findings and discuss the possible functional consequences of GABA$_B$Rs in development and maintenance of auditory brainstem function.

Mature expression pattern

GABA$_B$R1 expression appears as dense punctate label in mature NM, NA, and NL, but not the SON, where the label density is low. High expression in these areas suggests GABA$_B$Rs are likely to confer robust physiological functions in each of the targets of the GABAergic SON neurons, but perhaps not in the SON itself. Several anatomical and physiological studies have demonstrated the potent and robust GABAergic projections from SON to all of the brainstem auditory nuclei (Carr et al., 1989; Lachica et al., 1994; Yang et al., 1999, Burger et al., 2005). Two previous studies elegantly describe the role of GABA$_B$Rs in presynaptic modulation of glutamatergic nVIII input to NM (Brenowitz et al., 1998; Brenowitz and Trussell, 2001). Activation of these receptors appears important for preserving reliable synaptic transmission during high-frequency firing at this synapse.

The autoreceptor role of GABA$_B$Rs on GABAergic terminals is a common role of GABA$_B$Rs in the vertebrate nervous system (Misgeld et al., 1995). Our own recent study suggests a similar presynaptic function for GABA$_B$Rs on the GABAergic terminals in NM (Lu et al., 2004). Additionally, we recently demonstrated that individual SON neurons innervate multiple target nuclei among NM, NA, and NL (Burger et al., 2005). These results, taken together with the strong labeling observed in NA and NL in addition to NM, suggest that GABA$_B$Rs are also likely to presynaptically modulate GABAergic input to both NA and NL. We speculate that one function of GABA$_B$ autoregulation in NM is to preserve the phase-locking required for low-frequency binaural processing (Lu et al., 2004). The relative lack of GABA$_B$R labeling in SON may be a further indication that the separate commissural inhibitory pathway between the two SONs does not utilize and maintain

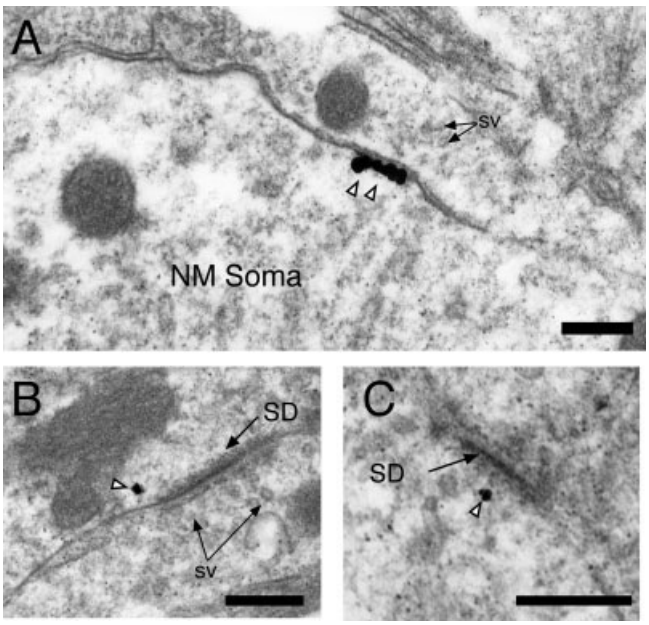

Fig. 9. Transmission electron photomicrographs confirm postsynaptic $GABA_BR$-I in NM. **A:** Several silver-enhanced gold particles aligned along the NM soma membrane closely apposed to a putative Type II synaptic profile. **B,C:** Silver-enhanced gold particles (white arrowheads) associated with postsynaptic densities (SD) suggestive of glutamatergic synaptic contacts in NM. sv, synaptic vesicles. Scale bars = 0.2 μm.

the precise temporal information seen in other regions of the brainstem auditory system (see Burger et al., 2005).

We did not observe a tonotopic gradient of $GABA_BR$ expression in NM or NL, in contrast to the reported tonotopic gradient in density of GABAergic terminals. Code et al. (1989) observed that GABA immunoreactivity is highest in the low-frequency region of NM and systematically decreases along the tonotopic dimension of the nucleus. The lack of a gradient of $GABA_BRs$ corresponding to the apparent input gradient underscores the slow kinetics of GABAergic signaling in NM and NL. In contrast to the unusually rapid glutamatergic conductances, the GABAergic kinetics are especially slow in these nuclei (Funabiki et al., 1998; Yang et al., 1999; Lu and Trussell, 2000; Monsivais et al., 2000). The slow kinetics result from a number of factors, including the coupling of $GABA_A$ responses to voltage-gated conductances and asynchronous release due to Ca^{++} accumulation in GABAergic terminals (Lu and Trussell, 2000; Monsivais et al., 2000; Monsivais and Rubel, 2001). Thus, it is not surprising that the density of kinetically slow $GABA_BRs$ does not vary along the tonotopic axis. These observations reinforce the notion that the time scale for GABAergic signaling in NM and NL is related to the general process of system gain rather than cycle-by-cycle modulation of phase-locked responses.

Development

We observed $GABA_BR1$ expression at very early developmental ages. $GABA_BR1$ immunoreactivity was apparent by E10. Expression at these ages precedes the expression of $GABA_A$ receptors and the observation of innervation by glutamic acid decarboxylase or GABA immunoreactive fibers (Code et al., 1989; Code and Churchill, 1991). The diffuse somatic staining present before E8–11 transitioned to punctate label at later ages. By E14, when GABAergic terminals are evident by GABA immunoreactivity, labeling for $GABA_BR1$ was dense in all four nuclei examined. The immunoreactivity remained high into maturity in all nuclei except the SON.

The diffuse somatic staining observed at early ages might reflect expression prior to functional recruitment to the membrane. Previous studies have shown functional $GABA_BRs$ are composed of a heterodimer of both a $GABA_BR1$ and a $GABA_BR2$ subunit (Jones et al., 1998; Kaupmann et al., 1998; White et al., 1998). Furthermore, $GABA_BR2$ subunit expression is required to recruit $GABA_BR1s$ to the membrane (Couve et al., 1998; Kuner et al., 1999; Margeta-Mitrovic et al., 2000). Thus, an appealing hypothesis is that a pool of $GABA_BR1$ subunits is generated prior to GABAergic innervation and is then recruited to the membrane as inhibitory synapses are forming. Additionally, the presence of $GABA_BR1$ expression prior to innervation suggests that the $GABA_BRs$ are well situated to provide a regulatory role in synaptogenesis. Recent studies in the superior olive of mammals demonstrate developmentally restricted synaptic plasticity of inhibitory inputs that is $GABA_BR$-dependent (Chang et al., 2003; Kotak and Sanes, 2003). The GABAergic innervation to the SON has not been well characterized. However, transient high expression of $GABA_BRs$ in the SON during the period of GABAergic innervation of the other brainstem nuclei suggests that $GABA_BRs$ may also developmentally regulate the reciprocal innervation of the SONs.

Deafferentation

In animals that underwent deafferentation by basilar papilla and ganglion cell removal, a slight decrease in immunoreactivity was observed in NM, but overall, robust $GABA_BR$ labeling remained. The small change associated with deprivation suggests that the overall contribution of the afferent nVIII terminals to the $GABA_BR$-I is relatively small despite the strong modulatory effect of $GABA_BRs$ on vesicle release from these terminals (Brenowitz et al., 1998; Brenowitz and Trussell, 2001). Thus, it appears that a sizeable portion of the remaining $GABA_BRs$ is expressed postsynaptically in addition to those expressed on inhibitory terminals. We confirmed postsynaptic expression by EM analysis of immunogold-reacted tissue.

The postsynaptic expression of $GABA_BR1$ is associated with both putative excitatory and inhibitory synaptic profiles, consistent with other studies (Kulik et al., 2003; Lujan et al., 2004). The consequences of this expression at both glutamatergic and GABAergic synapses are not entirely clear at present. Typically, postsynaptic $GABA_BRs$ are positively coupled to G-protein–coupled inwardly rectifying K^+ channels and reduce the excitability of cells (Kerr and Ong, 1995; Misgeld et al., 1995; Calver et al., 2002). Previous studies have shown that $GABA_BRs$ interact with metabotropic glutamate receptor signaling pathways in both hippocampal and Purkinje neurons (Hirono et al., 2001; Patenaude et al., 2003). Indeed, this laboratory has recently demonstrated a robust function in Ca^{++} homeostasis regulation by metabotropic glutamate receptors in NM that appears to interact with $GABA_B$ signaling pathways (Lu and Rubel, 2004; and unpubl. obs.). Thus,

further physiological investigation of the function of postsynaptic $GABA_B$Rs is necessary to test their involvement in regulating excitability or Ca^{++} currents in NM neurons.

CONCLUDING REMARKS

This study is the first, to our knowledge, to anatomically demonstrate and characterize the prevalent expression of $GABA_B$Rs in the avian auditory brainstem. The pervasive expression in the mature system, with the notable exception of the SON, and the variation in expression through development suggest that $GABA_B$Rs may serve multiple functions in the developing and mature system. It is our hope that these findings will stimulate further investigation into $GABA_B$ receptor function during development and in the mature auditory system.

ACKNOWLEDGMENTS

The authors thank Dale Cunningham for assistance with processing tissue for EM and for his ongoing dedication to this research program. We thank Glen MacDonald for expert assistance with microscopy in our center.

LITERATURE CITED

Benke D, Honer M, Michel C, Mohler H. 1996. $GABA_A$ receptor subtypes differentiated by their gamma-subunit variants: prevalence, pharmacology and subunit architecture. Neuropharmacology 35:1413–1423.

Born DE, Rubel EW. 1985. Afferent influences on brain stem auditory nuclei of the chicken: neuron number and size following cochlea removal. J Comp Neurol 231:435–445.

Brenowitz S, Trussell LO. 2001. Minimizing synaptic depression by control of release probability. J Neurosci 21:1857–1867.

Brenowitz S, David J, Trussell L. 1998. Enhancement of synaptic efficacy by presynaptic GABA(B) receptors. Neuron 20:135–141.

Burger RM, Cramer KS, Pfeiffer JD, Rubel EW. 2005. The avian superior olivary nucleus provides divergent inhibitory input to parallel auditory pathways. J Comp Neurol 481:6–18

Calver AR, Davies CH, Pangalos M. 2002. GABA(B) receptors: from monogamy to promiscuity. Neurosignals 11:299–314.

Carr CE, Fujita I, Konishi M. 1989. Distribution of GABAergic neurons and terminals in the auditory system of the barn owl. J Comp Neurol 286:190–207.

Chang EH, Kotak VC, Sanes DH. 2003. Long-term depression of synaptic inhibition is expressed postsynaptically in the developing auditory system. J Neurophysiol 90:1479–1488.

Code RA, Churchill L. 1991. $GABA_A$ receptors in auditory brainstem nuclei of the chick during development and after cochlea removal. Hear Res 54:281–295.

Code RA, Burd GD, Rubel EW. 1989. Development of GABA immunoreactivity in brainstem auditory nuclei of the chick: ontogeny of gradients in terminal staining. J Comp Neurol 284:504–518.

Conlee JW, Parks TN. 1986. Origin of ascending auditory projections to the nucleus mesencephalicus lateralis pars dorsalis in the chicken. Brain Res 367:96–113.

Couve A, Filippov AK, Connolly CN, Bettler B, Brown DA, Moss SJ. 1998. Intracellular retention of recombinant $GABA_B$ receptors. J Biol Chem 273:26361–26367.

Fritschy JM, Meskenaite V, Weinmann O, Honer M, Benke D, Mohler H. 1999. $GABA_B$-receptor splice variants GB1a and GB1b in rat brain: developmental regulation, cellular distribution and extrasynaptic localization. Eur J Neurosci 11:761–768.

Fukui I, Ohmori H. 2004. Tonotopic gradients of membrane and synaptic properties for neurons of the chicken nucleus magnocellularis. J Neurosci 24:7514–7523.

Funabiki K, Koyano K, Ohmori H. 1998. The role of GABAergic inputs for coincidence detection in the neurones of nucleus laminaris of the chick. J Physiol 508(Pt 3):851–869.

Hausler UH, Sullivan WE, Soares D, Carr CE. 1999. A morphological study of the cochlear nuclei of the pigeon *(Columba livia)*. Brain Behav Evol 54:290–302.

Hirono M, Yoshioka T, Konishi S. 2001. GABA(B) receptor activation enhances mGluR-mediated responses at cerebellar excitatory synapses. Nat Neurosci 4:1207–1216.

Hyson RL, Reyes AD, Rubel EW. 1995. A depolarizing inhibitory response to GABA in brainstem auditory neurons of the chick. Brain Res 677: 117–126.

Jhaveri S, Morest DK. 1982. Sequential alterations of neuronal architecture in nucleus magnocellularis of the developing chicken: a Golgi study. Neuroscience 7:837–853.

Jones KA, Borowsky B, Tamm JA, Craig DA, Durkin MM, Dai M, Yao WJ, Johnson M, Gunwaldsen C, Huang LY, Tang C, Shen Q, Salon JA, Morse K, Laz T, Smith KE, Nagarathnam D, Noble SA, Branchek TA, Gerald C. 1998. GABA(B) receptors function as a heteromeric assembly of the subunits GABA(B)R1 and GABA(B)R2. Nature 396:674–679.

Kaupmann K, Malitschek B, Schuler V, Heid J, Froestl W, Beck P, Mosbacher J, Bischoff S, Kulik A, Shigemoto R, Karschin A, Bettler B. 1998. GABA(B)-receptor subtypes assemble into functional heteromeric complexes. Nature 396:683–687.

Kerr DI, Ong J. 1995. $GABA_B$ receptors. Pharmacol Ther 67:187–246.

Kotak VC, Sanes DH. 2003. Gain adjustment of inhibitory synapses in the auditory system. Biol Cybern 89:363–370.

Kulik A, Vida I, Lujan R, Haas CA, Lopez-Bendito G, Shigemoto R, Frotscher M. 2003. Subcellular localization of metabotropic GABA(B) receptor subunits GABA(B1a/b) and GABA(B2) in the rat hippocampus. J Neurosci 23:11026–11035.

Kuner R, Kohr G, Grunewald S, Eisenhardt G, Bach A, Kornau HC. 1999. Role of heteromer formation in $GABA_B$ receptor function. Science 283: 74–77.

Lachica EA, Rubsamen R, Rubel EW. 1994. GABAergic terminals in nucleus magnocellularis and laminaris originate from the superior olivary nucleus. J Comp Neurol 348:403–418.

Lu Y, Rubel E. 2005. Activation of metabotropic glutamate receptors inhibits high voltage-gated calcium channel currents of chicken nucleus magnocellularis neurons. J Neurophysiol 93:1418–1428.

Lu T, Trussell LO. 2000. Inhibitory transmission mediated by asynchronous transmitter release. Neuron 26:683–694.

Lu T, Trussell LO. 2001. Mixed excitatory and inhibitory GABA-mediated transmission in chick cochlear nucleus. J Physiol 535:125–131.

Lu Y, Burger RM, Rubel EW. 2005. $GABA_B$ receptor activation modulates $GABA_A$ receptor mediated inhibition in chicken nucleus magnocellularis neurons. J Neurophysiol 93:1429–1438.

Lujan R, Shigemoto R, Kulik A, Juiz JM. 2004. Localization of the $GABA_B$ receptor 1a/b subunit relative to glutamatergic synapses in the dorsal cochlear nucleus of the rat. J Comp Neurol 475:36–46.

Margeta-Mitrovic M, Jan YN, Jan LY. 2000. A trafficking checkpoint controls GABA(B) receptor heterodimerization. Neuron 27:97–106.

Misgeld U, Bijak M, Jarolimek W. 1995. A physiological role for $GABA_B$ receptors and the effects of baclofen in the mammalian central nervous system. Prog Neurobiol 46:423–462.

Monsivais P, Rubel EW. 2001. Accommodation enhances depolarizing inhibition in central neurons. J Neurosci 21:7823–7830.

Monsivais P, Yang L, Rubel EW. 2000. GABAergic inhibition in nucleus magnocellularis: implications for phase locking in the avian auditory brainstem. J Neurosci 20:2954–2963.

Otis TS, Trussell LO. 1996. Inhibition of transmitter release shortens the duration of the excitatory synaptic current at a calyceal synapse. J Neurophysiol 76:3584–3588.

Owens DF, Kriegstein AR. 2002. Is there more to GABA than synaptic inhibition? Nat Rev Neurosci 3:715–727.

Parks TN, Rubel EW. 1975. Organization and development of brain stem auditory nuclei of the chicken: organization of projections from n. magnocellularis to n. laminaris. J Comp Neurol 164:435–448.

Patenaude C, Chapman CA, Bertrand S, Congar P, Lacaille JC. 2003. $GABA_B$ receptor- and metabotropic glutamate receptor-dependent cooperative long-term potentiation of rat hippocampal $GABA_A$ synaptic transmission. J Physiol 553:155–167.

Rubel EW. 1978. Ontogeny of structure and function in the vertebrate auditory system. In: Jacobson M, editor. Handbook of sensory physiology. Berlin: Springer. p 135–237.

Rubel EW, Parks TN. 1975. Organization and development of brain stem

auditory nuclei of the chicken: tonotopic organization of n. magnocellularis and n. laminaris. J Comp Neurol 164:411–433.

Rubel EW, Parks TN. 1988. The developing auditory system. In: Edelman GM, editor. Auditory function. New York: John Wiley & Sons. p 3–91.

Rubel EW, Parks TN, Zirpel L. 2004. Assembling, connecting, and maintaining the cochlear nucleus. In: Parks TN, Rubel EW, Popper AN, Fay RR, editors. Plasticity in the auditory system. Berlin: Springer Science and Business Media. p 8–48.

Soares D, Carr CE. 2001. The cytoarchitecture of the nucleus angularis of the barn owl (*Tyto alba*). J Comp Neurol 429:192–205.

Soares D, Chitwood RA, Hyson RL, Carr CE. 2002. Intrinsic neuronal properties of the chick nucleus angularis. J Neurophysiol 88:152–162.

von Bartheld CS, Code RA, Rubel EW. 1989. GABAergic neurons in brainstem auditory nuclei of the chick: distribution, morphology, and connectivity. J Comp Neurol 287:470–483.

Warchol ME, Dallos P. 1990. Neural coding in the chick cochlear nucleus. J Comp Physiol [A] 166:721–734.

Westerberg BD, Schwarz DW. 1995. Connections of the superior olive in the chicken. J Otolaryngol 24:20–30.

White JH, Wise A, Main MJ, Green A, Fraser NJ, Disney GH, Barnes AA, Emson P, Foord SM, Marshall FH. 1998. Heterodimerization is required for the formation of a functional GABA(B) receptor. Nature 396:679–682.

Yang L, Monsivais P, Rubel EW. 1999. The superior olivary nucleus and its influence on nucleus laminaris: a source of inhibitory feedback for coincidence detection in the avian auditory brainstem. J Neurosci 19:2313–2325.